

Double parton interactions as a background to associated HW production at the Tevatron

Dmitry Bandurin¹, Georgy Golovanov², Nikolai Skachkov²

¹ *Department of Physics, Florida State University, Tallahassee, FL 32306*

² *Joint Institute for Nuclear Research, Dubna, Russia, Joliot-Curie 6, 141980*

Abstract

In this paper we study events with W +jets final state, produced in double parton (DP) interactions, as a background to the associated Higgs boson (H) and W production, with $H \rightarrow b\bar{b}$ decay, at the Tevatron. We have found that the event yield from the DP background can be quite sizable, which necessitates a choice of selection criteria to separate the HW and DP production processes. We suggest a set of variables sensitive to the kinematics of DP and HW events. We show that these variables, being used as an input to the artificial neural network, allow one to significantly improve a sensitivity to the Higgs boson production.

I. INTRODUCTION

A significant amount of experimental data, ranging from ISR energies [1] through the SPS [2] to the Tevatron [3–8], and even to photoproduction at HERA [9, 10], shows clear evidence of hard jets produced from multiple parton interactions (MPI). Specifically, in the Tevatron Run I and Run II studies, 4-jet [3] and $\gamma + 3$ -jet events [4, 7] have been considered with jet $p_T \gtrsim 5 - 15$ GeV, and the fraction of events occurring due to double parton (DP) interactions have been measured. Those fractions varied depending on the final state and the jet transverse momentum (p_T) of the second parton interaction. The fraction measured using 4-jet final state is found to be 5.5% for jet $p_T > 25$ GeV [3]. The fractions obtained from the $\gamma + 3$ -jet production range from 51.3% for the second (ordered in p_T) and third jet p_T in the interval $5 - 7$ GeV¹ [4] to 47% – 22% for the second jet p_T within $15 - 30$ GeV [7].

Those experiments have also measured the effective cross section σ_{eff} , an important parameter that contains information about the parton spatial density inside the (anti)proton: $\sigma_{\text{eff}} = 12.1^{+10.7}_{-5.4}$ mb in the 4-jet production in CDF [3], $\sigma_{\text{eff}} = 14.5 \pm 1.7^{+1.7}_{-2.3}$ mb and $\sigma_{\text{eff}} = 16.4 \pm 0.3 \pm 2.3$ mb in the $\gamma + 3$ -jet productions in CDF [4] and D0 [7], respectively. This parameter allows the calculation of a DP cross section σ_{DP} for any pair of partonic processes A and B according to:

$$\sigma_{DP} \equiv m \frac{\sigma^A \sigma^B}{\sigma_{\text{eff}}}. \quad (1)$$

The factor m has a Poissonian nature [11] and should be equal to 1/2 for two indistinguishable processes (like two dijet productions in A and B) or gives unity for distinguishable processes. The CDF [4] and D0 [7] experiments obtained the most accurate results on σ_{eff} with an average value of about $\sigma_{\text{eff}}^{\text{ave}} = 15.5$ mb.

In addition to information about parton spatial structure, those studies also pointed out that the DP interactions can be a noticeable background to many rare processes, especially for those with multijet final state. In this case an additional partonic interaction, producing most likely a dijet final state, can mimic the multijet signal signature. Some estimates of the DP background to the Higgs boson production processes at the LHC have been done in [12–15].

In this paper we consider the DP events, caused by the W +dijet production, as a background to the HW production, with $W \rightarrow l\nu$ and $H \rightarrow b\bar{b}$ decays, which is one of the most promising Higgs boson search channels at the Tevatron. An example of a possible DP process with $W + b\bar{b}$ production is shown in figure 1. However, in addition to the two- b -jet final state produced in the second parton scattering, we also expect significant contribution from final states with light+heavy flavor and two light jets.

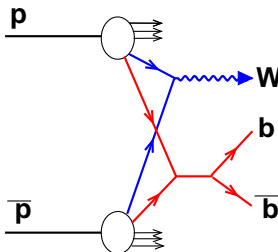


Figure 1: A possible diagram for $W + b\bar{b}$ production due to DP scattering.

Due to the similarity of HW and HZ final states, we expect that the relative DP background from Z +dijet production to the HZ events should be quite close to the HW case. For this reason, we limit our study to DP background to the HW events only.

This paper is organized as follows. In section II we describe how DP and Higgs boson samples are simulated and selected. In section III we calculate differential cross sections $d\sigma/dM_{jj}$ (where M_{jj} is the invariant mass of the two leading jets) and event yields in the HW and DP processes including the jet energy detector smearing and b -jet identification effects. The rates of events with $W+2$ -jet production due to the DP and conventional single parton (SP) scatterings are compared in section IV. In section V we introduce a set of variables sensitive to the kinematics of the signal $HW(Z)$ and DP background final states and use them as an input to a dedicated Artificial Neural Network (ANN) to separate the two event types. We make our conclusions in section VI.

¹ In this measurement jet p_T is raw, i.e. uncorrected for the energy losses [4].

II. SIMULATION AND SELECTIONS

A. Selections

The current PYTHIA event generator [16] is the best framework to study many effects related to MPI production. It includes a few sophisticated phenomenological models which consider the MPI scatterings with their various correlations, including parton momentum and color. The MPI models in PYTHIA 6, have been tuned to experimental results, and reproduce many observables in data quite well [11, 17]. PYTHIA 8, which inherited the majority of features of its predecessor, also allows the combination of different kinds of parton processes in the first (main) and second scatterings within kinematic regions of interest. To simulate events for the study we used PYTHIA 8 with Tune 2C as an MPI model². The HW production channel simulated with Higgs boson masses of $m_H = 115$ and 150 GeV was considered. The DP scattering was simulated as inclusive $q\bar{q} \rightarrow W + X$ production in the first parton process and inclusive QCD dijet production in the second process. To increase statistics in the selected final states with the cuts above, the W scattering process is required to have invariant mass $50 < m_W < 120$ GeV and the minimal allowed parton transverse momentum (\hat{p}_\perp^{min}) in the dijet process is required to be $\hat{p}_\perp^{min} = 10$ GeV.

The event selection criteria are taken from [18] and applied to both, the HW and DP production events and briefly summarized below:

- The Higgs boson is required to decay into $b\bar{b}$.
- The W-boson is selected in the electron and muon decay modes with lepton $p_T > 15$ GeV and pseudorapidity $|\eta| < 1.1$ or $1.5 < |\eta| < 2.5$ for electrons and $|\eta| < 1.6$ for muons.
- The total vector sum \vec{p}_T of neutrinos should be > 20 GeV (an approximate analog of missing $E_T > 20$ GeV in [18]).
- At least two jets are required with $p_T > 20$ GeV and $|\eta| < 2.5$. Jets are found by the D0 Run II midpoint cone algorithm with radius $R=0.5$ [19]. For this aim we used the FASTJET package [20] interfaced to PYTHIA 8.
- The scalar sum of the jet transverse momenta (HT) is required to be $HT > 60$ GeV for the 2 jet final state and $HT > 80$ GeV for the 3 jet one.

B. Normalizations

The cross sections of the simulated events were normalized to either experimentally measured cross sections or to theoretical NNLO predictions. Specifically, we normalized all the PYTHIA cross sections in the following way:

- We simulated dijet events production and calculated cross sections in the dijet mass bins 150 – 175 and 175 – 200 GeV, and the two rapidity regions of $|y| < 0.4$ and $0.4 < |y| < 0.8$ available from the recent D0 measurement [21]. We have found that a required PYTHIA-to-data correction factor (“K-factor”) is about 1.26, approximately valid for both the dijet mass bins and the two rapidity regions.
- We also simulated separately W inclusive production and, from a comparison of its cross section with the D0 and CDF measurements [22, 23], have obtained a PYTHIA-to-data K-factor of about 1.5.
- The HW cross section has been normalized to the NNLO predictions [24] with the PYTHIA-to-NNLO K-factor equal to 1.45.
- We corrected the effective cross section σ_{eff} used in Tune 2C³ by a factor 1.6 to match the CDF and D0 measurements [4, 7] with averaged result $\sigma_{\text{eff}}^{\text{ave}} = 15.5$ mb.

The uncertainty assigned in our analysis to the K-factors are 10% and 16% to $\sigma_{\text{eff}}^{\text{ave}}$. The latter is due to the difference between the D0 and CDF σ_{eff} central values ($\sim 7\%$) and the systematic uncertainties ($\sim 14\%$) in the D0 measurement.

III. $d\sigma/dM_{jj}$ CROSS SECTIONS FOR HW AND DOUBLE PARTON EVENTS

A. HW and DP cross sections

In this section we calculate the differential cross sections $d\sigma/dM_{jj}$ for the HW and DP (W +dijet) events selected according to the criteria of section II. To match the detector resolution, the jet transverse momenta p_T are smeared

² This tune was suggested by the PYTHIA authors.

³ The effective cross section σ_{eff} in PYTHIA 8 is taken as a ratio of a total non-diffractive cross section to an impact-parameter enhancement factor, depending on the parton spatial density distribution.

using

$$\frac{\sigma_{p_T}}{p_T} = \frac{S}{\sqrt{p_T}} \oplus C, \quad (2)$$

where $S = 0.75$ and $C = 0.06$ which approximately reproduces the jet p_T resolution for the D0 detector [25]. The differential cross sections $d\sigma/dM_{jj}$ for the HW and DP productions including the smearing effect are shown in figure 2. In addition to the total DP cross section, contributions from the main DP scattering subprocesses are also shown in a separate plot. One can see from these two plots that (a) the DP cross section dominates the HW signal by more than two orders of magnitude, and (b) the DP cross section is caused mainly by the $W+2$ light jets (stemming from $u/d/s$ -quarks or gluons) production, followed, in the order of importance, by contributions from $W + gc$, $W + gb$, and then by $W + c\bar{c}$ and $W + b\bar{b}$ events.

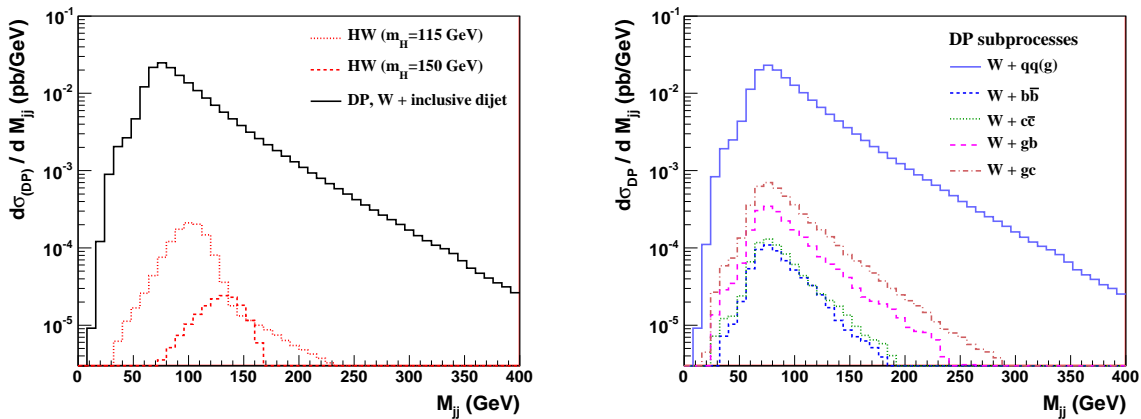


Figure 2: The differential cross sections in the dijet mass M_{jj} bins for signal HW and background DP events including the jet p_T resolution. On the left plot, dotted and dash-dotted red lines correspond to HW events with $m(H) = 115$ and 150 GeV, respectively, while the full black line shows the total background from all the DP W +dijet channels. The right plot shows contributions from main parton scattering subprocesses composing the total DP background.

B. Account of b -jet identification efficiencies

In the signal HW events we have two b jets in the final state. Since the leading DP background is caused by the $W+2$ light jet events (figure 2), we should expect a significant reduction after requiring of jet b -tagging. To check this numerically, we apply a specific b -tagging requirement for the HW and DP events. In our fast MC we cannot check the jet b -tagging quality, but we instead use the efficiencies to pass the b -tagging requirements for light (l), c and b jets. We take these efficiencies from [26], where they are parametrized as functions of jet p_T and η . These efficiencies are used to re-weight events according to the jet flavors. Typical efficiencies are 50 – 70% for b -jets, 8 – 12% for c -jets and 0.5 – 2% for l -jets. The variations reflect dependence on the jet p_T , η and tightness of the b -tagging condition. We consider a given jet to be a b -jet if it has a b -quark in the jet cone; if the jet does not have a b -quark but has a c -quark instead, it is considered to be a c -jet; otherwise it is a light jet. Figure 3 shows the cross sections $\times b$ -jet identification efficiency ($\epsilon_{b-id}^{\text{jet}}$) for the DP and HW events, where each of the two jets is required to satisfy the “loose” b -tagging requirement [26]. This requirement significantly suppresses rates of the DP events. However, the signal rates are also noticeably reduced (compare figures 2 and 3). For this reason, in practice, double tagging is usually combined with single tagging. For example, in the search for HW signal [18], two cases of the b -tagging are considered: either an event should contain two jets satisfying “loose” b -tagging requirements or, if it fails, a single jet should satisfy the “tight” requirement. Fractions of background (=data) and the HW events selected with the single b -tagging can be taken from [18]: they are about 85% and 60% correspondingly⁴. The remaining events are with two b -tagged jets.

⁴ Clearly, here we assume that the jet flavor content of the background events in data and the dijet events from the DP interaction is the same. However, we believe that for the current level of estimates this assumption should be good enough.

Figure 4 shows the cross sections $\times \epsilon_{b-id}^{jet}$ for the DP and HW events where we have combined events with single and

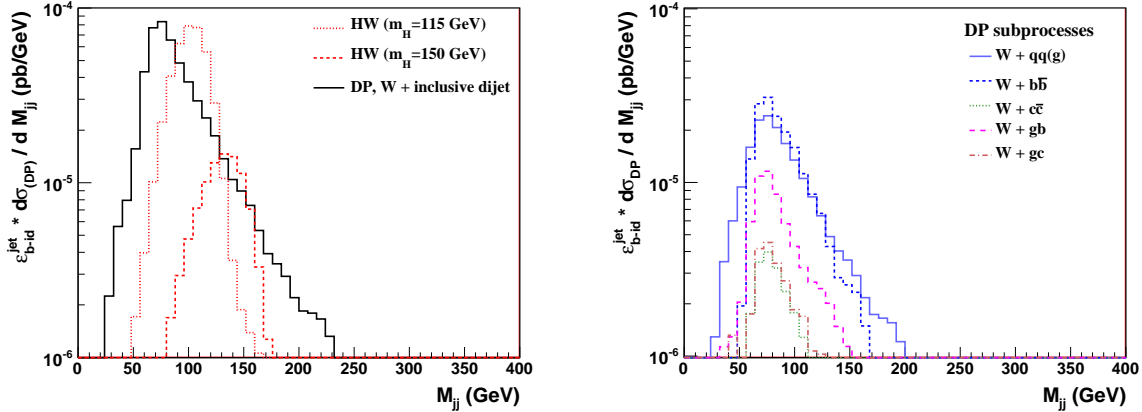


Figure 3: The differential cross sections in the dijet mass bins for signal HW and background DP events including the jet p_T resolution and requirement of the two jet b -tagging (See also description in the caption to figure 2).

double b -tagging according to their fractions mentioned above. We see that while the dominating DP channel is still caused by the $W+2$ light jet production, the relative contribution from $W + gb$ production is now much higher than in figure 2 (no b -tagging is applied). The $W + gb$ contribution is followed by similar ones from the $W + gc$ and $W + b\bar{b}$ events.

Figure 5 is complementary to figure 4 and shows the ratios of the HW event yield to the inclusive DP W +dijet one in the dijet mass M_{jj} bins for the events selected by the combined b -tagging. The uncertainty in each bin is caused by the K-factors and effective cross section (section II).

One can see that the Higgs boson events with $m_H = 115$ GeV are expected to be suppressed by about a factor 3 ($S/B \simeq 0.35$) in the peak position, while the signal events with $m_H = 150$ GeV are suppressed by about a factor 7.

It is interesting to compare the total number of the signal events predicted by our fast MC after all selections (figure 4) with those in [18] for the integrated luminosity $L_{int} = 5.3 \text{ fb}^{-1}$. It is obtained by integrating the cross section over the whole M_{jj} range (20–400 GeV) and multiplying by L_{int} . In such a way we have found the expected signal statistics of about 31 (7) events for $m_H = 115$ (150) GeV. According to [18] there should be about 19 ± 1 selected events for $m_H = 115$ GeV. Our estimate seems to be in a reasonable agreement if we take into account the effects of finite lepton identification, jet taggability efficiencies, and detector acceptance unaccounted in our fast MC.

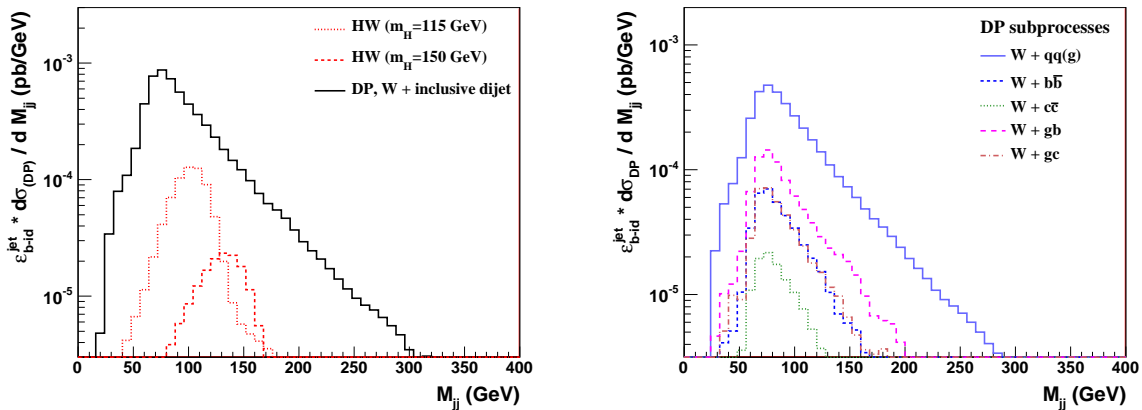


Figure 4: The differential cross sections in the dijet mass bins for signal HW and background DP events including the jet p_T resolution and the combined jet b -tagging efficiency (see also the main text and the caption to figure 2).

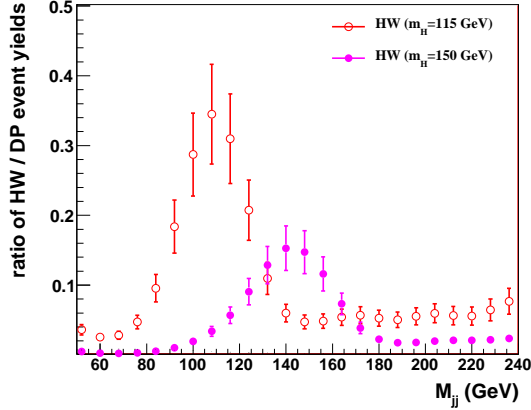


Figure 5: The ratio of HW signal to DP background event yields with the combined b -tagging (see the main text).

IV. COMPARISON OF THE DP AND SP EVENT YIELDS

In this section we compare the event yields dN/dM_{jj} expected for the DP and SP $W+2$ -jet productions. The two additional jets in the SP events come from radiation effects in the initial and/or final states. SP events are simulated using $q\bar{q} \rightarrow Wg$ and $qg \rightarrow Wq$ subprocesses and applying the HW selection criteria from section II. To reproduce the inclusive $W+2$ jet cross section in data [27], the PYTHIA events are reweighted with a scaling factor depending on the second jet p_T , what increases the PYTHIA $W+2$ jet cross section in the region $110 < M_{jj} < 160$ GeV by about a factor 2. Also, as before, the jet p_T is smeared according to the p_T resolution, eq. (2) and the events are weighted with the jet b -tagging efficiencies according to the jet flavors.

The estimated total event yields in the whole mass region at $L_{int} = 5.3 \text{ fb}^{-1}$ for SP and DP events are about 5212 and 262 events, respectively. The differential ratios of the DP/SP $W+2$ -jet event yields in the M_{jj} bins are shown in figure 6. They are about 5 – 8% for $M_{jj} \simeq 115$ GeV and 3.5 – 6% for $M_{jj} \simeq 150$ GeV.

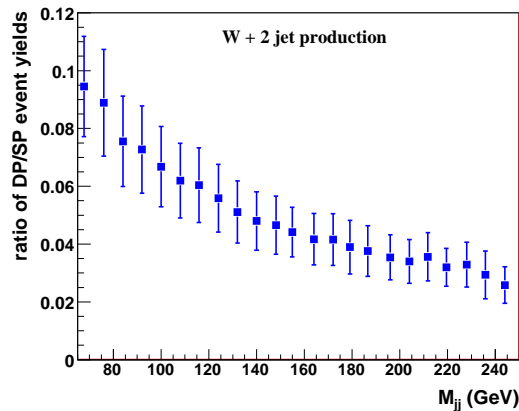


Figure 6: The ratio of the DP to SP event yields for the $W+2$ -jet production.

V. ARTIFICIAL NEURAL NETWORK FOR DP AND HW(Z) SEPARATION

A. Variables

In this section we discuss variables that can be useful to separate the $HW(Z)$ signal from the DP $W(Z)$ +dijet background events. Most of these variables are either based on the previous relevant experimental studies [1–7] or have been suggested in theoretical papers [11, 28–34]. Due to the similarity of HW and HZ events, most of these variables should be useful to suppress the DP background events to both the final states (with some exclusions). Definitions of all the variables are summarized below.

- The first variable is an azimuthal angle between two p_T vectors, where the first one corresponds to the $W(Z)$ p_T vector, while the second one is a sum of the leading and second jet p_T vectors:

$$\Delta S \equiv \Delta\phi(\vec{p}_T[V], \vec{p}_T[\text{jet}_1, \text{jet}_2]), \quad (3)$$

where $\vec{p}_T[V]$ is the transverse momentum vector of $V(=W, Z)$ -boson and $\vec{p}_T[\text{jet}_1, \text{jet}_2] = \vec{p}_T^{\text{jet}_1} + \vec{p}_T^{\text{jet}_2}$. For historical reasons [1–4, 7] we call this angle ΔS .

- The second variable is the difference between the rapidity of the V -boson and the total rapidity of the two-jet system:

$$\Delta\eta(V, \text{jet}12) = |\eta^V - (\eta^{\text{jet}1} + \eta^{\text{jet}2})|. \quad (4)$$

- The variable $\Delta\eta(V, \text{jet}12)$ can be calculated just for $V = Z$ events, but not for W due to the missing p_z information of the ν . Instead we can use the rapidity of the electron (e) η^e from the W decay and introduce an analogous variable:

$$\Delta\eta(e, \text{jet}12) = |\eta^e - (\eta^{\text{jet}1} + \eta^{\text{jet}2})|. \quad (5)$$

- In the case of the W production the azimuthal angle between the electron from the W decay and the leading jet $\Delta\phi(e, \text{jet}1)$ can be considered.

Two other variables use angular differences between the first and second jets:

- the azimuthal angle between the jets $\Delta\phi(\text{jet}1, \text{jet}2)$.
- the difference between rapidities of the first and second jets $\Delta\eta(\text{jet}1, \text{jet}2)$.
- Another variable characterizes the orientation of the two event planes, one contains the beam (proton) axis and V -boson, and the other one contains the two jets [35]:

$$\cos\psi^*(V, \text{jet}12) = \frac{(\vec{p}^V \times \vec{p}^{\text{proton}}) \cdot (\vec{p}^{\text{jet}1} \times \vec{p}^{\text{jet}2})}{|\vec{p}^V \times \vec{p}^{\text{proton}}| \cdot |\vec{p}^{\text{jet}1} \times \vec{p}^{\text{jet}2}|}. \quad (6)$$

- In the case of the W production, we do not have the 3-vector of the W momentum but can use the electron 3-vector instead, i.e. we should calculate $\cos\psi^*(e, \text{jet}12)$.

Three other variables are based on the jet p_T :

- the total sum of the first and second jet p_T :

$$p_T^{\text{sum}12} = p_T^{\text{jet}1} + p_T^{\text{jet}2}. \quad (7)$$

- the relative difference between the first and second jet p_T :

$$p_T^{\text{diff}12} = (p_T^{\text{jet}1} - p_T^{\text{jet}2})/p_T^{\text{sum}12}. \quad (8)$$

- the total p_T sum of all jets, p_T^{sumAll} .
- Finally, we add the total number of all jets ($p_T > 6$ GeV), N_{jets} .

All these 12 variables are shown in figures 7 and 8 for HW and DP W +dijet events. They demonstrate a good separation power between the two event types.

B. ANN

The variables presented above can be used as input to a dedicated ANN to separate the HW from the DP events. The variable p_T^{sumAll} is very correlated with $p_T^{\text{sum}12}$, but the latter is a bit more sensitive to the signal/background difference. We do not use the dijet mass information to minimize dependence on a specific Higgs boson mass region but rather concentrate on other more generic kinematic properties of the two event types.

We have chosen the following 9 variables to train the ANN: ΔS , $\Delta\eta(e, \text{jet}12)$, $\Delta\phi(e, \text{jet}1)$, $\Delta\phi(\text{jet}1, \text{jet}2)$, $\Delta\eta(\text{jet}1, \text{jet}2)$, $\cos\psi^*(e, \text{jet}12)$, $p_T^{\text{sum}12}$, $p_T^{\text{diff}12}$, and N_{jets} , using the package JETNET [36]. The ANN is trained using the signal HW (simulated with $m_H = 115$ GeV) and background DP events to produce a single output value equal to zero for the background and unity for the signal events. The DP background events for the training (and later for testing) purposes are selected around the Higgs boson M_{jj} peak position taking all events within $\pm 2\sigma$ around the peak. We have trained the ANN using 200,000 the signal and background events and then tested the ANN using 50,000 events that have not been used at the training stage. The normalized distributions of the signal and background events for the ANN output O_{NN} is presented in figure 9. The ANN weights obtained at the training stage, have been used later to also separate the HW signal simulated with $m_H = 150$ GeV and DP events.

Tighter cuts on the ANN output will reject a larger fraction of the DP events. Figure 10 shows the correlation between efficiencies to select the background and signal events ($\varepsilon_b^{\text{ANN}}$ and $\varepsilon_s^{\text{ANN}}$, respectively) for the two Higgs boson masses, $m_H = 115$ GeV and $m_H = 150$ GeV. Selecting 90% (80%) of the signal events with $m_H = 115$ GeV we will keep only about 24% (13%) of the DP events, while selecting 90% (80%) of the signal events with $m_H = 150$ GeV we will keep about 9% (4%) of the DP events.

C. Results

The built ANN is used to further suppress the DP background, which strongly dominates the signal events even after the b-tagging selections (figure 5). The new signal-to-background ratios are shown in two plots of figure 11, corresponding to the choice of the HW signal efficiencies $\varepsilon_s^{\text{ANN}} = 90\%$ and 80% . The ratios at $\varepsilon_s^{\text{ANN}} = 90\%$ for both the mass regions, 115 GeV and 150 GeV, are now close to 1.3 – 1.5. This ratio grows further with $\varepsilon_s^{\text{ANN}} = 80\%$, and reaches about 2.2 at $M_{jj} \simeq 115$ GeV and about 2.7 at $M_{jj} \simeq 150$ GeV.

VI. CONCLUSION

In our current study we have shown that the W +dijet events produced due to the DP scattering can compose a quite sizable background to the associated HW production with $H \rightarrow b\bar{b}$ decay. Its relative fraction with respect to the traditional background from SP scattering with the W +2-jet final state is found to be 4 – 8% in the dijet mass region $115 < M_{jj} < 150$ GeV. We suggest a set of the angular and jet p_T variables that are sensitive to the difference between the HW and DP kinematics. The neural network built using these variables allows significant suppression of the DP background to a desirable level. Provided that the overall systematics in the Higgs searches in the HW channel will go down in a time and since every percent of the background events matters, use of the suggested anti-DP neural network should be very helpful.

Acknowledgments

The authors thank Wade Fisher and Aurelio Juste for useful discussions and Stephen Mrena for the help with use of the PYTHIA 8 code.

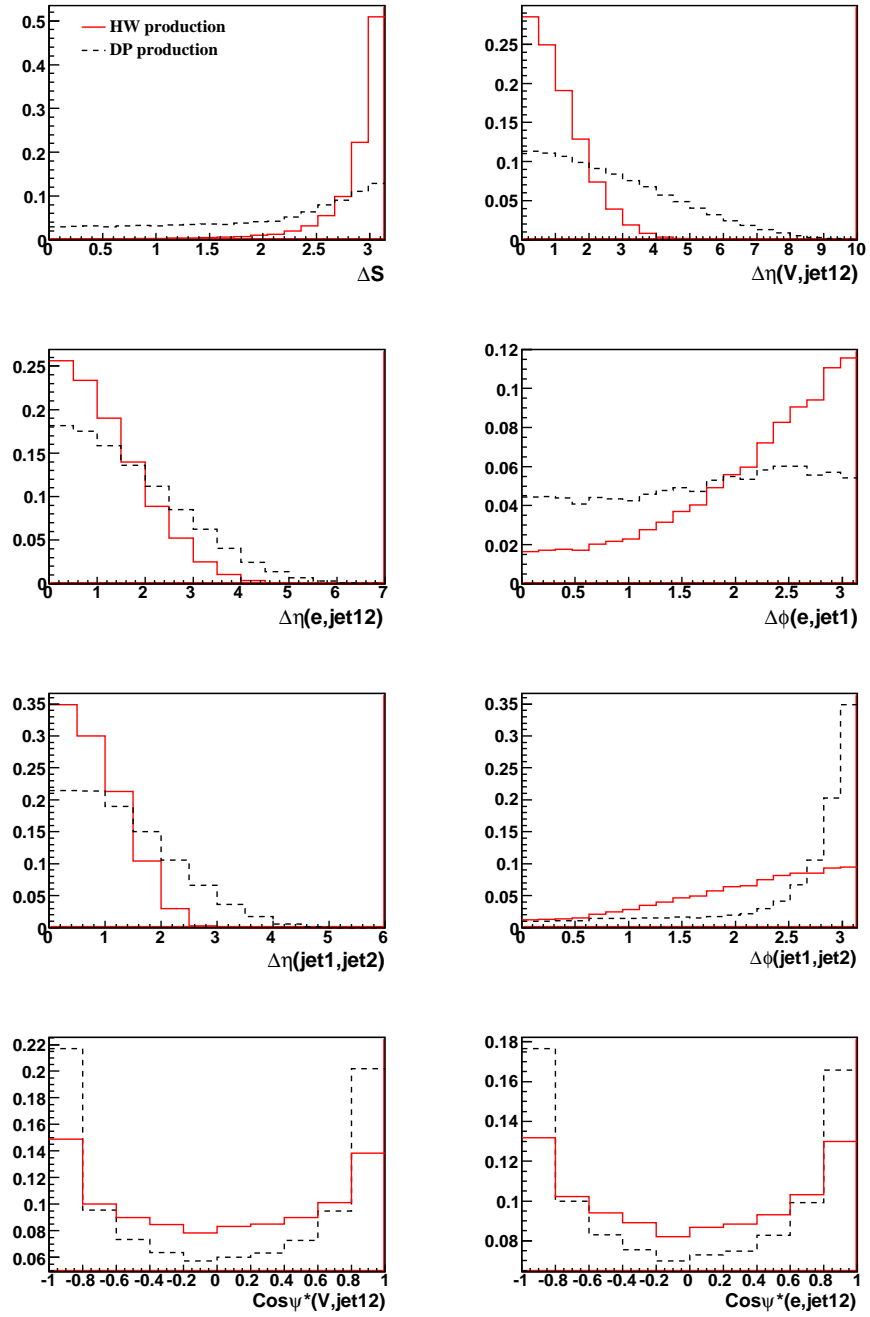


Figure 7: Normalized distributions of the number of HW signal (full red line) and W +dijets background (dashed black line) events over the kinematic variables of section V A (part 1).

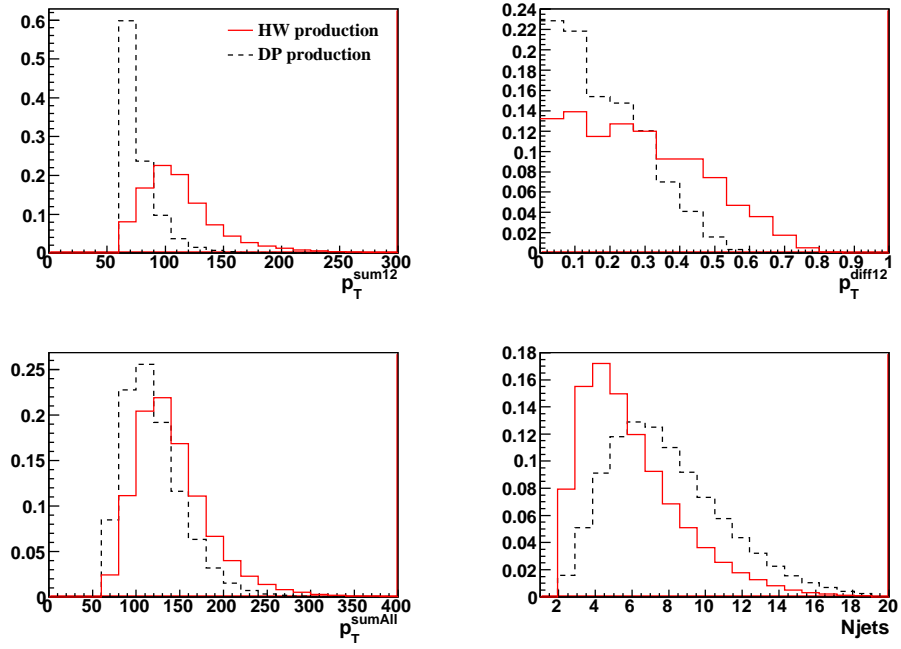


Figure 8: Normalized distributions of the number of HW signal (full red line) and W +dijets background (dashed black line) events over the kinematic variables of section V A (part 2).

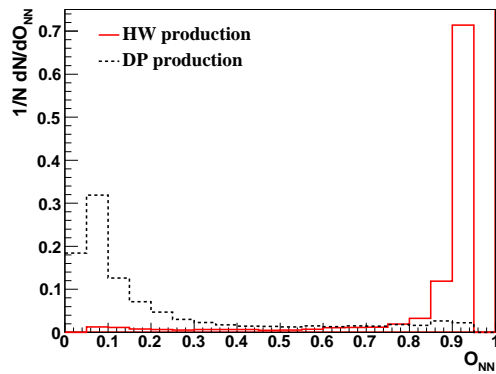


Figure 9: The ANN output for the DP and HW ($m_H = 115$ GeV) events using the 9 input variables described in the text.

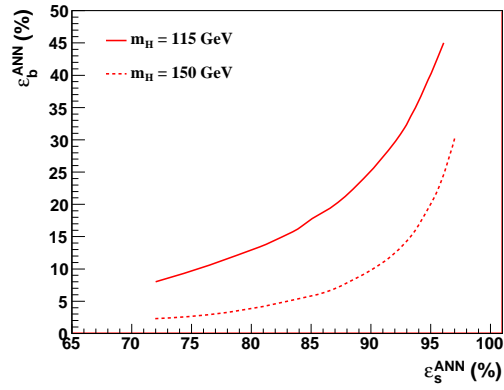


Figure 10: DP versus HW neural network selection efficiencies.

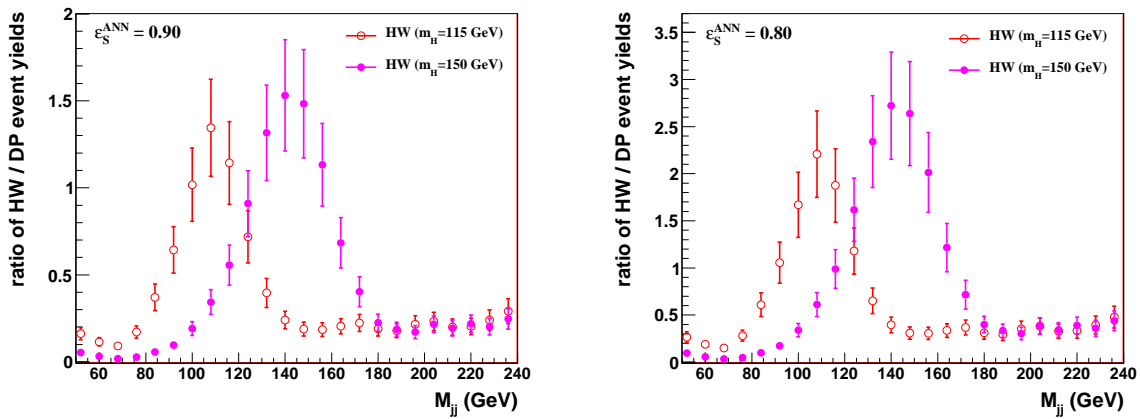


Figure 11: Ratio of the HW event yields to the DP ones with account of the ANN selection efficiencies taken for the HW events to be 90% on the left and 80% on the right plot.

-
- [1] **Axial Field Spectrometer** Collaboration, T. Akesson *et. al.*, *Double parton scattering in pp collisions at $\sqrt{s} = 63$ GeV*, *Z. Phys.* **C34** (1987) 163.
- [2] **UA2** Collaboration, J. Alitti *et. al.*, *A Study of multi-jet events at the CERN $p\bar{p}$ collider and a search for double parton scattering*, *Phys. Lett.* **B268** (1991) 145–154.
- [3] **CDF** Collaboration, F. Abe *et. al.*, *Study of four jet events and evidence for double parton interactions in $p\bar{p}$ collisions at $\sqrt{s} = 1.8$ TeV*, *Phys. Rev.* **D47** (1993) 4857–4871.
- [4] **CDF** Collaboration, F. Abe *et. al.*, *Double parton scattering in $p\bar{p}$ collisions at $\sqrt{s} = 1.8$ TeV*, *Phys. Rev.* **D56** (1997) 3811–3832.
- [5] **E735** Collaboration, T. Alexopoulos *et. al.*, *The role of double parton collisions in soft hadron interactions*, *Phys. Lett.* **B435** (1998) 453–457.
- [6] **D0** Collaboration, V. M. Abazov *et. al.*, *Multiple jet production at low transverse energies in $p\bar{p}$ collisions at $\sqrt{s} = 1.8$ TeV*, *Phys. Rev.* **D67** (2003) 052001, [hep-ex/0207046].
- [7] **D0** Collaboration, V. M. Abazov *et. al.*, *Double parton interactions in photon+3 jet events in $p\bar{p}$ collisions at $\sqrt{s} = 1.96$ TeV*, *Phys. Rev.* **D81** (2010) 052012, [arXiv:0912.5104].
- [8] **D0** Collaboration, V. M. Abazov *et. al.*, *Azimuthal decorrelations and multiple parton interactions in photon+2 jet and photon+3 jet events in $p\bar{p}$ collisions at $\sqrt{s} = 1.96$ TeV*, Submitted to *Phys. Rev. D* (2011) [arXiv:1101.1509].
- [9] **ZEUS** Collaboration, C. Gwenlan, *Multijets in photoproduction at HERA*, *Acta Phys. Polon.* **B33** (2002) 3123–3128.
- [10] **H1** Collaboration, F. D. Aaron, *Study of multiple interactions in photoproduction at HERA*, H1-prelim-08-036.
- [11] T. Sjostrand and M. van Zijl, *A Multiple Interaction Model for the Event Structure in Hadron Collisions*, *Phys. Rev.* **D36** (1987) 2019.
- [12] A. Del Fabbro and D. Treleani, *A double parton scattering background to Higgs boson production at the LHC*, *Phys. Rev.* **D61** (2000) 077502, [hep-ph/9911358].
- [13] A. Del Fabbro and D. Treleani, *Double parton scatterings in b-quark pairs production at the LHC*, *Phys. Rev.* **D66** (2002) 074012, [hep-ph/0207311].
- [14] M. Y. Hussein, *Double parton scattering in associate Higgs boson production with bottom quarks at hadron colliders*, [arXiv:0710.0203].
- [15] E. L. Berger, C. B. Jackson, and G. Shaughnessy, *Characteristics and Estimates of Double Parton Scattering at the Large Hadron Collider*, *Phys. Rev.* **D81** (2010) 014014, [arXiv:0911.5348].
- [16] T. Sjostrand, S. Mrenna, and P. Z. Skands, *PYTHIA 6.4 Physics and Manual*, *JHEP* **05** (2006) 026, [hep-ph/0603175].
- [17] T. Sjostrand and P. Z. Skands, *Multiple interactions and the structure of beam remnants*, *JHEP* **03** (2004) 053, [hep-ph/0402078].
- [18] **D0** Collaboration, V. M. Abazov *et. al.*, *Search for WH associated production with 5.3 fb⁻¹ of RunII data*, Submitted to *Phys. Lett. B* (2010) [arXiv:1012.0874].
- [19] G. C. Blazey *et. al.*, *Run II jet physics*, [hep-ex/0005012].
- [20] M. Cacciari and G. P. Salam, *Dispelling the N³ myth for the k_t jet-finder*, *Phys. Lett.* **B641** (2006) 57–61, [hep-ph/0512210].
- [21] **D0** Collaboration, V. M. Abazov *et. al.*, *Measurement of the dijet invariant mass cross section in proton anti-proton collisions at $\sqrt{s} = 1.96$ TeV*, *Phys. Lett.* **B693** (2010) 531–538, [arXiv:1002.4594].
- [22] **D0** Collaboration, V. M. Abazov *et. al.*, *Measurement of the cross section for W and Z production to electron final state with the D0 detector at $\sqrt{s} = 1.96$ TeV*, <http://www-d0.fnal.gov/Run2Physics/WWW/results/prelim/EW/E06/E06.pdf>.
- [23] **CDF** Collaboration, D. Acosta *et. al.*, *First measurements of inclusive W and Z cross sections from Run II of the Tevatron collider*, *Phys. Rev. Lett.* **94** (2005) 091803, [hep-ex/0406078].
- [24] T. Hahn, S. Heinemeyer, F. Maltoni, G. Weiglein, and S. Willenbrock, *SM and MSSM Higgs boson production cross sections at the Tevatron and the LHC*, [hep-ph/0607308].
- [25] **D0** Collaboration, V. M. Abazov *et. al.*, *Measurement of the inclusive jet cross-section in $p\bar{p}$ collisions at $\sqrt{s} = 1.96$ TeV*, *Phys. Rev. Lett.* **101** (2008) 062001, [arXiv:0802.2400].
- [26] **D0** Collaboration, V. M. Abazov *et. al.*, *b-Jet Identification in the D0 Experiment*, *Nucl. Instrum. Meth.* **A620** (2010) 490–517, [arXiv:1002.4224].
- [27] **CDF** Collaboration, T. Aaltonen *et. al.*, *Measurement of the cross section for W-boson production in association with jets in $p\bar{p}$ collisions at $\sqrt{s} = 1.96$ TeV*, *Phys. Rev.* **D77** (2008) 011108(R), [arXiv:0711.4044].
- [28] P. V. Landshoff and J. C. Polkinghorne, *Calorimeter triggers for hard collisions*, *Phys. Rev.* **D18** (1978) 3344.
- [29] C. Goebel, F. Halzen, and D. M. Scott, *Double Drell-Yan annihilations in hadron collisions: novel tests of the constituent picture*, *Phys. Rev.* **D22** (1980) 2789.
- [30] F. Takagi, *Multiple production of quark jets off nuclei*, *Phys. Rev. Lett.* **43** (1979) 1296.
- [31] N. Paver and D. Treleani, *Multi - quark scattering and large P(T) jet production in hadronic collisions*, *Nuovo Cim.* **A70** (1982) 215.
- [32] B. Humpert, *Are there multi - quark interactions?*, *Phys. Lett.* **B131** (1983) 461.
- [33] B. Humpert and R. Odorico, *Multiparton scattering and QCD radiation as sources of four jet events*, *Phys. Lett.* **B154** (1985) 211.
- [34] M. L. Mangano, *Four Jet Production at the Tevatron Collider*, *Z. Phys.* **C42** (1989) 331.
- [35] **D0** Collaboration, S. Abachi *et. al.*, *Studies of Topological Distributions of the Three- and Four-Jet Events in $p\bar{p}$*

Collisions at $\sqrt{s} = 1800$ GeV with the D0 Detector, *Phys. Rev.* **D53** (1996) 6000–6016, [hep-ex/9509005].

- [36] C. Peterson, T. Rognvaldsson, and L. Lonnblad, *JETNET 3.0: A Versatile artificial neural network package*, *Comput. Phys. Commun.* **81** (1994) 185–220.